Electronic Supplementary Information

Novel $Al_2Mo_3O_{12}$-based temperature-stable microwave dielectric ceramics for LTCC applications

Junqing Ren[a,b], Ke Bi[a], Xiuli Fu[*a], Zhijian Peng[*b]

[a] *State Key Laboratory of Information Photonics and Optical Communications, and School of Science, Beijing University of Posts and Telecommunications, Beijing 100876, P. R. China*

[b] *School of Science, China University of Geosciences, Beijing 100083, P. R. China*

[*]Email: xiulifu@bupt.edu.cn. Tel: 86-10-62282242. Fax: 86-10-62282242.

[*]Email: pengzhijian@cugb.edu.cn. Tel: 86-10-82320255; Fax: 86-10-82323426.

Financial support from the National Natural Science Foundation of China (grant nos. 11674035 and 61274015), and Fund of State Key Laboratory of Information Photonics and Optical Communications (Beijing University of Posts and Telecommunications) is gratefully acknowledged.

Junqing Ren, et al., *Journal of Materials Chemistry C*, Figure S1

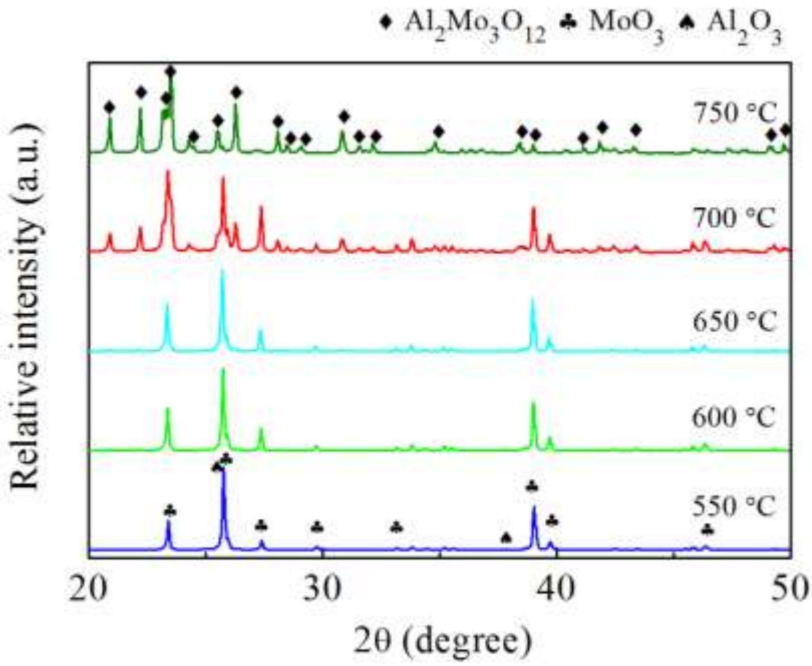

Figure S1 XRD patterns of the obtained $Al_2Mo_3O_{12}$ powders calcined at 550-750 °C for 4 h.

From Figure S1, it is seen that although for the sample prepared at the calcination temperature of 700 °C, $Al_2Mo_3O_{12}$ phase has been detected from the XRD patterns, Al_2O_3 and MoO_3 phases could still be identified from the patterns of the samples calcined at 550-700 °C, which are originating from the applied source powders. At the lowest synthesis temperature of 750 °C, pure $Al_2Mo_3O_{12}$ with monoclinic phase (JCPDS card no. 84-1652) could be obtained.

Junqing Ren, et al., *Journal of Materials Chemistry C*, Figure S2

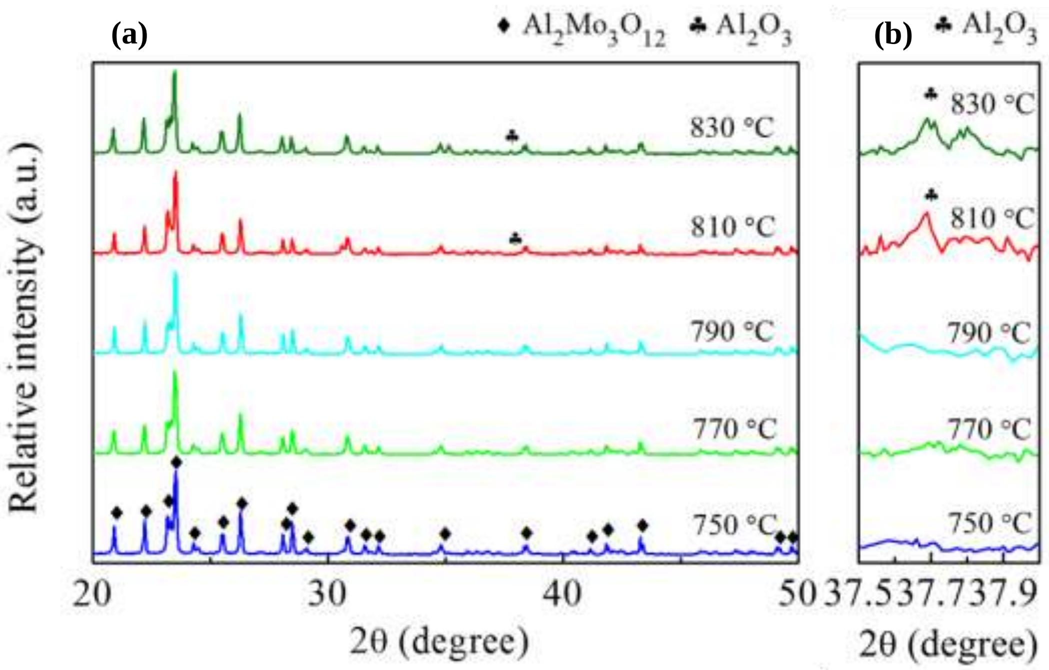

Figure S2 (a) XRD patterns of the obtained $Al_2Mo_3O_{12}$ ceramics sintered at 750-830 °C for 12 h, and (b) an elaborated observation on the diffraction peak around 37.7°.

It is seen in **Figure S2a** that, the main phase of all the samples is a monoclinic structure of $Al_2Mo_3O_{12}$ (JCPDS card no. 84-1652). However, through an elaborated observation on the characteristic diffraction peak at the 2θ angle around 37.7° (see **Figure S2b**), Al_2O_3 phase could be identified from the samples sintered at a temperature higher than 810 °C, because the volatilization of MoO_3 happens at such high sintering temperature, thus leaving Al_2O_3 in the samples alone.

Junqing Ren, et al., *Journal of Materials Chemistry C*, Figure S3

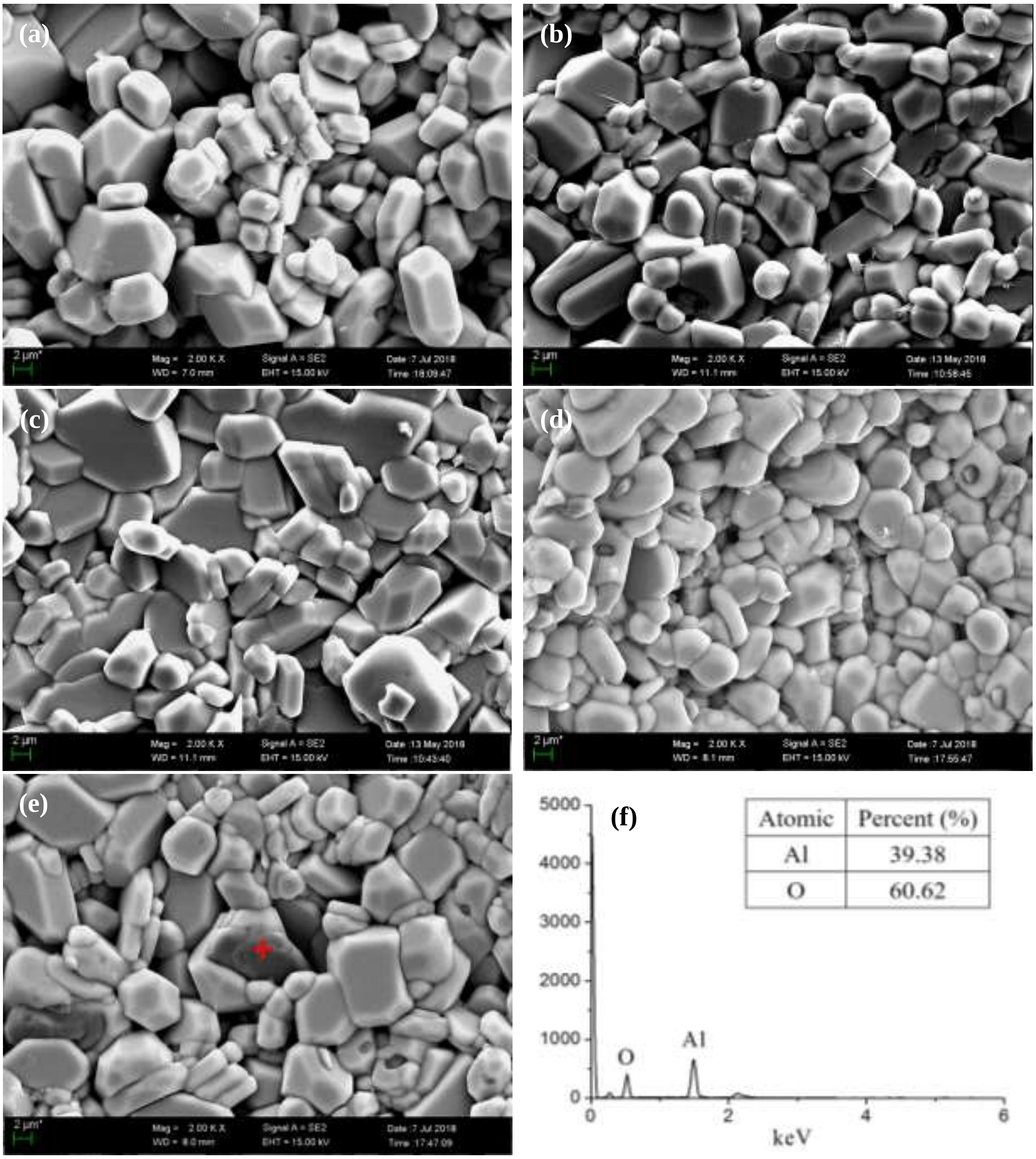

Figure S3 Typical SEM images of the obtained $Al_2Mo_3O_{12}$ ceramics sintered at different temperatures for 12 h: (a) 750, (b) 770, (c) 790, (d) 810 and (e) 830 °C. (f) EDX data on the marked grain in (e).

As is seen in **Figure S3**, when sintering at 750-770 °C, there exist inhomogeneously sized $Al_2Mo_3O_{12}$ grains and many pores in the samples, indicating that the sintering is not complete. At 790-830 °C, denser samples with more homogeneous grain size could be obtained. However, when sintering at 830 °C, some dark impurities consisting of Al_2O_3 appears in the samples together with the main $Al_2Mo_3O_{12}$ phase (see **Figure S3f**).

Junqing Ren, et al., *Journal of Materials Chemistry C*, Figure S4

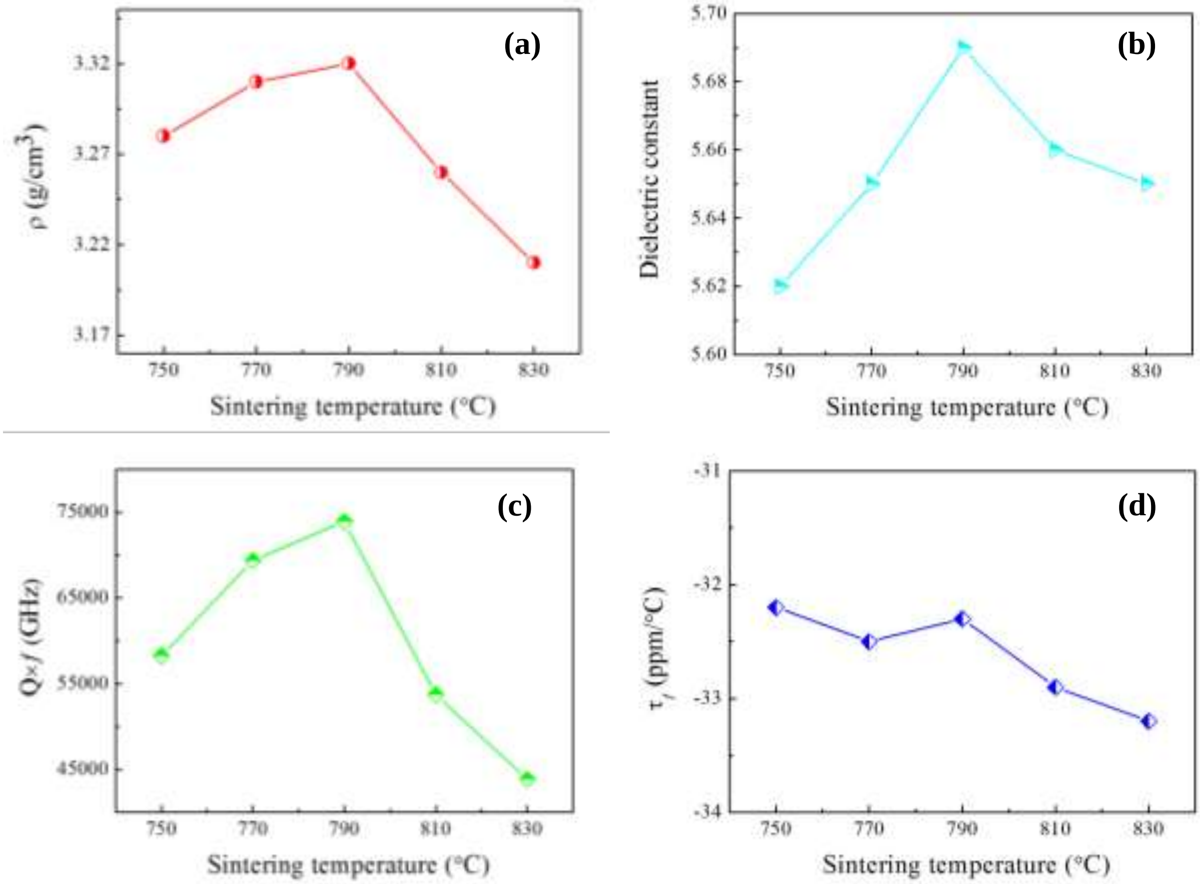

Figure S4 Apparent density (a), dielectric constant (b), quality factor (c) and temperature coefficient of resonant frequency (d) of the obtained $Al_2Mo_3O_{12}$ ceramics sintered at 750-830 °C for 12 h.

From **Figure S4**, it can be seen that the apparent density reaches the maximum when the sample is sintered at 790 °C. Meanwhile, the dielectric constant and quality factor of the obtained $Al_2Mo_3O_{12}$ ceramics reach their maximum value, respectively. The temperature coefficient of resonant frequency of the obtained ceramics decreased with increasing sintering temperature.

Junqing Ren, et al., *Journal of Materials Chemistry C*, Figure S5

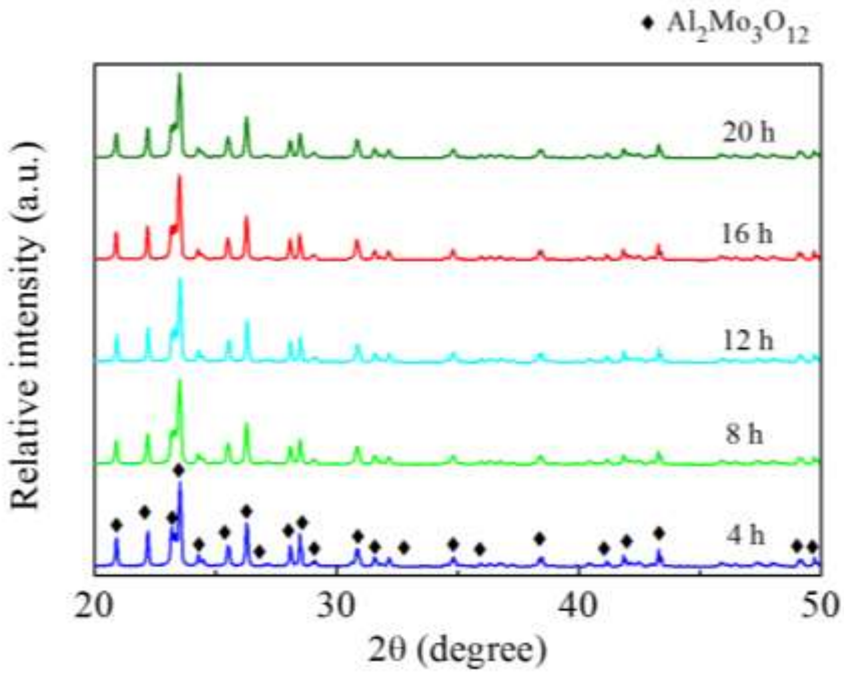

Figure S5 XRD patterns of the obtained $Al_2Mo_3O_{12}$ ceramics sintered at 790 °C for 4-20 h.

As is seen in **Figure S5,** a single phase of monoclinic $Al_2Mo_3O_{12}$ (JCPDS card no. 84-1652) could be detected in all the samples, and no obvious second phases could be identified, indicating that $Al_2Mo_3O_{12}$ phase in the samples was stable at 790 °C.

Junqing Ren, et al., *Journal of Materials Chemistry C*, Figure S6

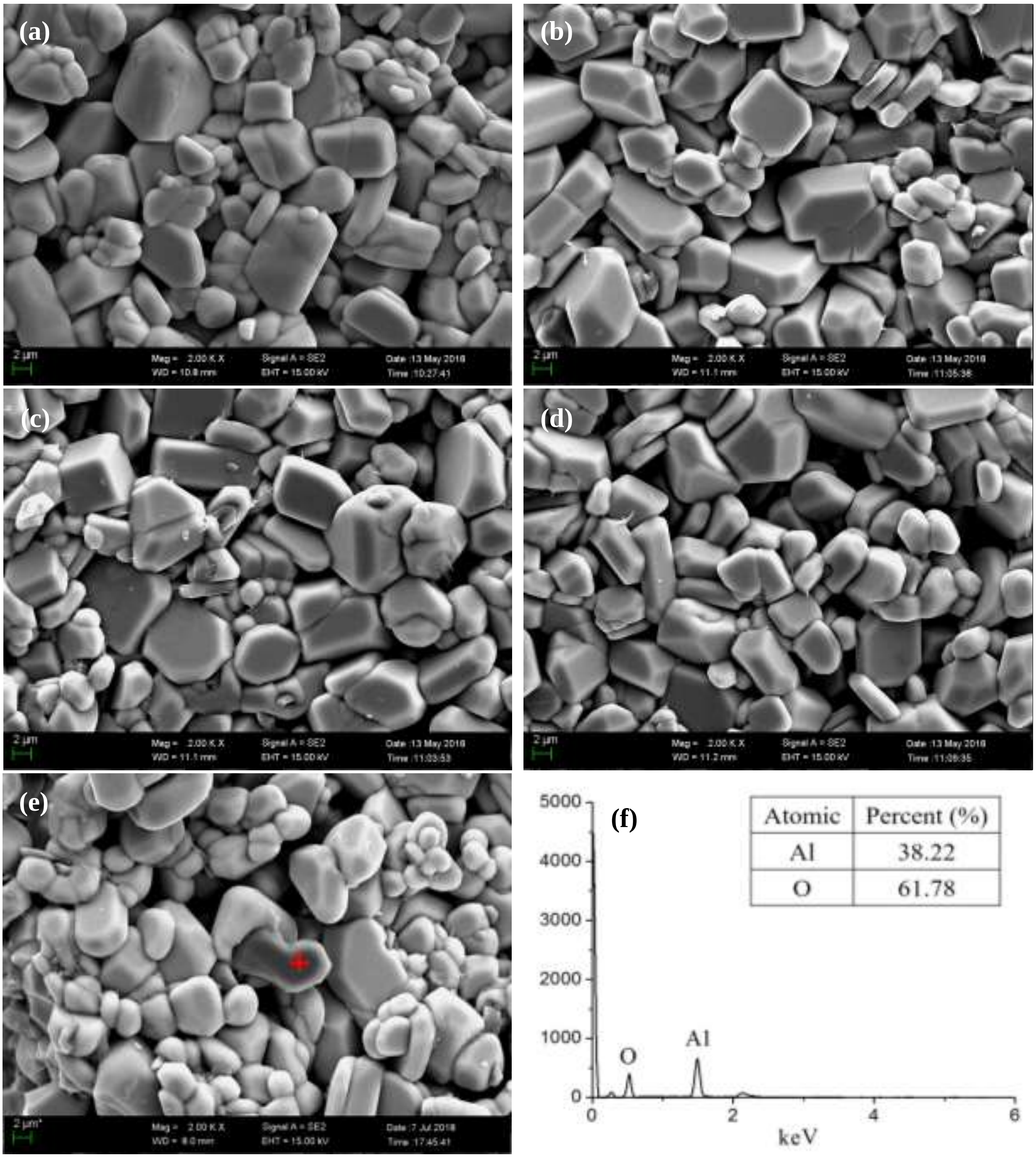

Figure S6 Typical SEM images of the obtained $Al_2Mo_3O_{12}$ ceramics sintered at 790 °C for different times: (a) 4, (b) 8, (c) 12, (d) 16 and (e) 20 h. (f) EDX data on the marked grain in (e).

As is seen in **Figure S6**, when sintering at 790 °C for 4-8 h, there exist inhomogeneously sized $Al_2Mo_3O_{12}$ grains and many pores in the samples, indicating that the sintering is not complete. For 12-16 h, denser samples with more homogeneous grain size could be obtained. However, when sintering for 20 h, some dark impurities consisting of Al_2O_3 appears in the samples together with the main $Al_2Mo_3O_{12}$ phase (see **Figure S6f**).

Junqing Ren, et al., ***Journal of Materials Chemistry C*****, Figure S7**

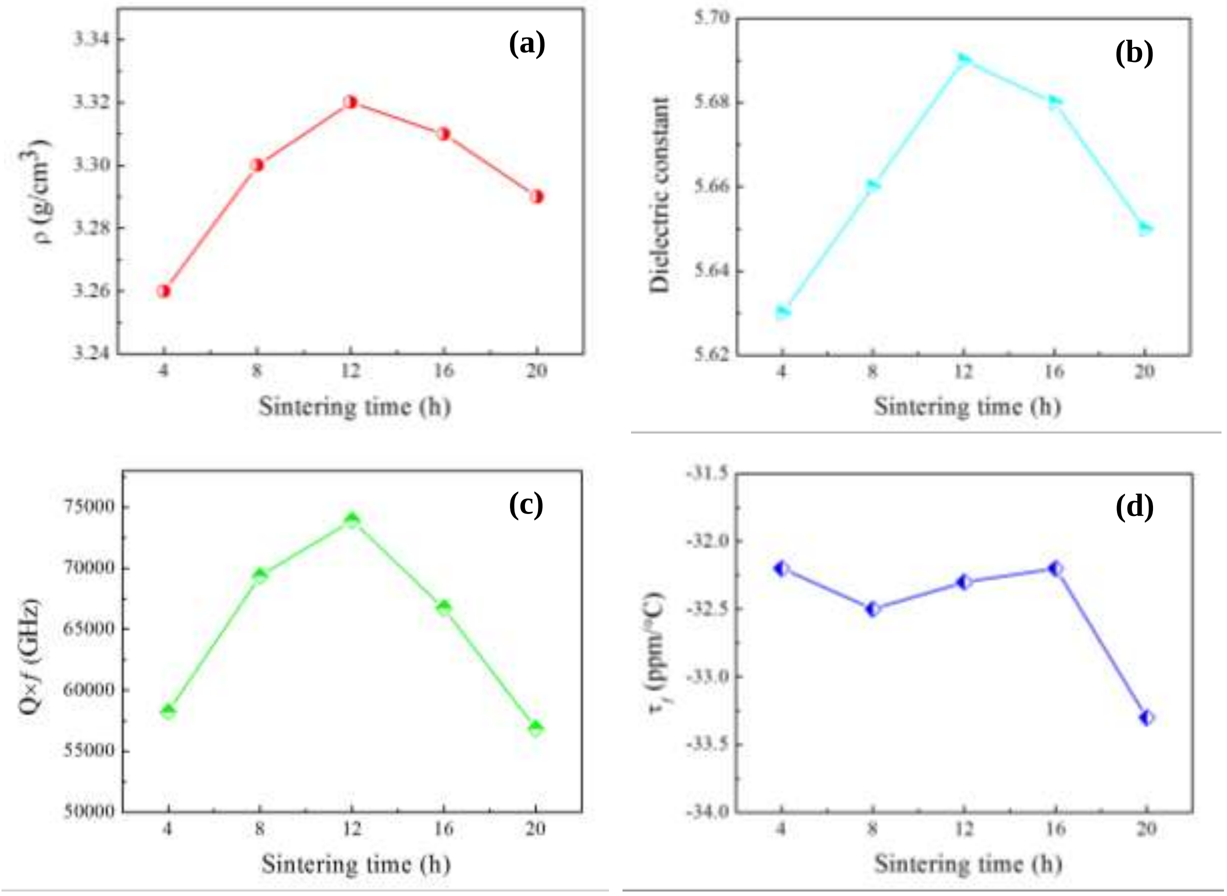

Figure S7 Apparent density (a), dielectric constant (b), quality factor (c) and temperature coefficient of resonant frequency (d) of the obtained $Al_2Mo_3O_{12}$ ceramics sintered at 790 °C for 4-20 h.

From **Figure S7**, it can be seen that the apparent density reaches the maximum when the sample is sintered for 12 h at 790 °C. Meanwhile, the dielectric constant and quality factor of the obtained $Al_2Mo_3O_{12}$ ceramics reach their maximum value, respectively. The temperature coefficient of resonant frequency of the obtained ceramics decreased with extending sintering time.

Junqing Ren, et al., *Journal of Materials Chemistry C*, Figure S8

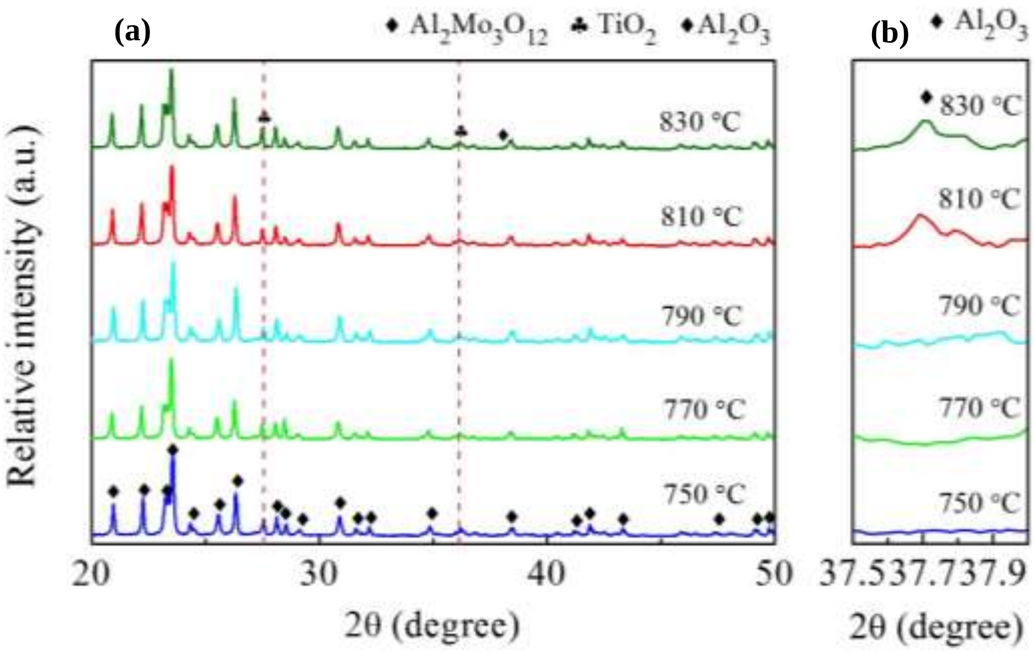

Figure S8 (a) XRD patterns of the obtained $0.6Al_2Mo_3O_{12}$-$0.4TiO_2$ ceramics sintered at 750-830 °C for 12 h, and (b) an elaborated observation on the diffraction peak around 37.7°.

From **Figure S8a,** it can be seen that monoclinic $Al_2Mo_3O_{12}$ (JCPDS card no. 84-1652) and rutile TiO_2 (JCPDS card no. 21-1276) phases could be detected in all the samples, indicating that TiO_2 could coexist with $Al_2Mo_3O_{12}$ phase. However, through an elaborated observation on the characteristic diffraction peaks at the 2θ angles around 37.7° (see **Figure S8b**), Al_2O_3 phase could be identified from the samples sintered at a temperature higher than 790 °C. Thus, from the point of phase composition, 790 °C was the optimized sintering temperature for $0.6Al_2Mo_3O_{12}$-$0.4TiO_2$ ceramics.

Junqing Ren, et al., *Journal of Materials Chemistry C*, Figure S9

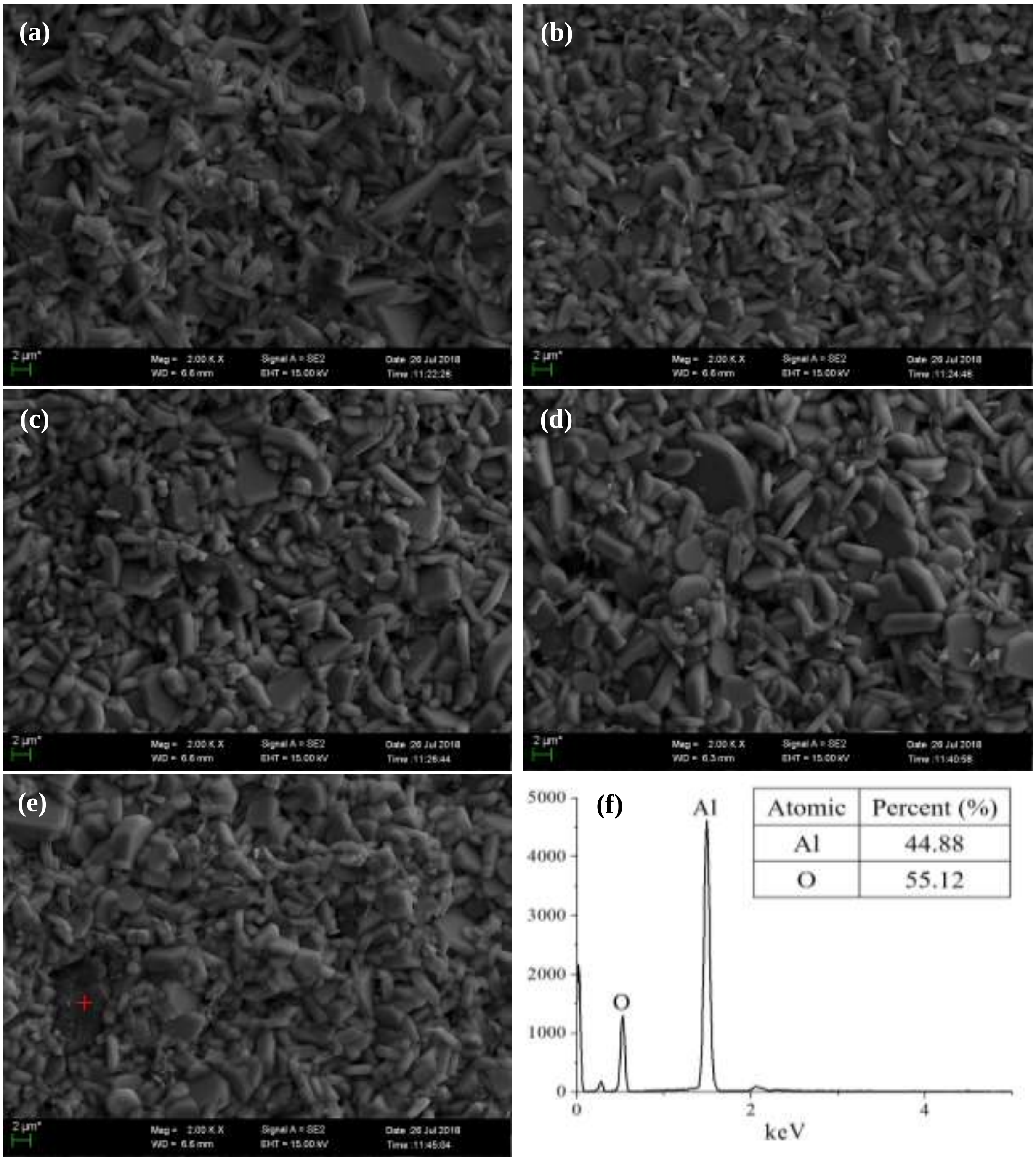

Figure S9 Typical SEM images of the obtained $0.6Al_2Mo_3O_{12}$-$0.4TiO_2$ ceramics sintered at different temperatures for 12 h: (a) 750, (b) 770, (c) 790 C, (d) 810 °C and (e) 830 °C. (f) EDX data on the marked grain in (e).

As is seen in **Figure S9(a-c)**, after adding TiO_2, the average grain size of $Al_2Mo_3O_{12}$ decreased. When sintering at a temperature below 790 °C, there exist inhomogeneously sized $Al_2Mo_3O_{12}$ grains and many pores in the samples, indicating that the sintering is not complete. At 790 °C, denser samples with more homogeneous grain size could be obtained. However, when sintering at a temperature higher than 790 °C, some dark impurities consisting of Al_2O_3 appears in the samples together with the main $Al_2Mo_3O_{12}$ phase (see **Figure S9e**).

Junqing Ren, et al., *Journal of Materials Chemistry C*, Figure S10

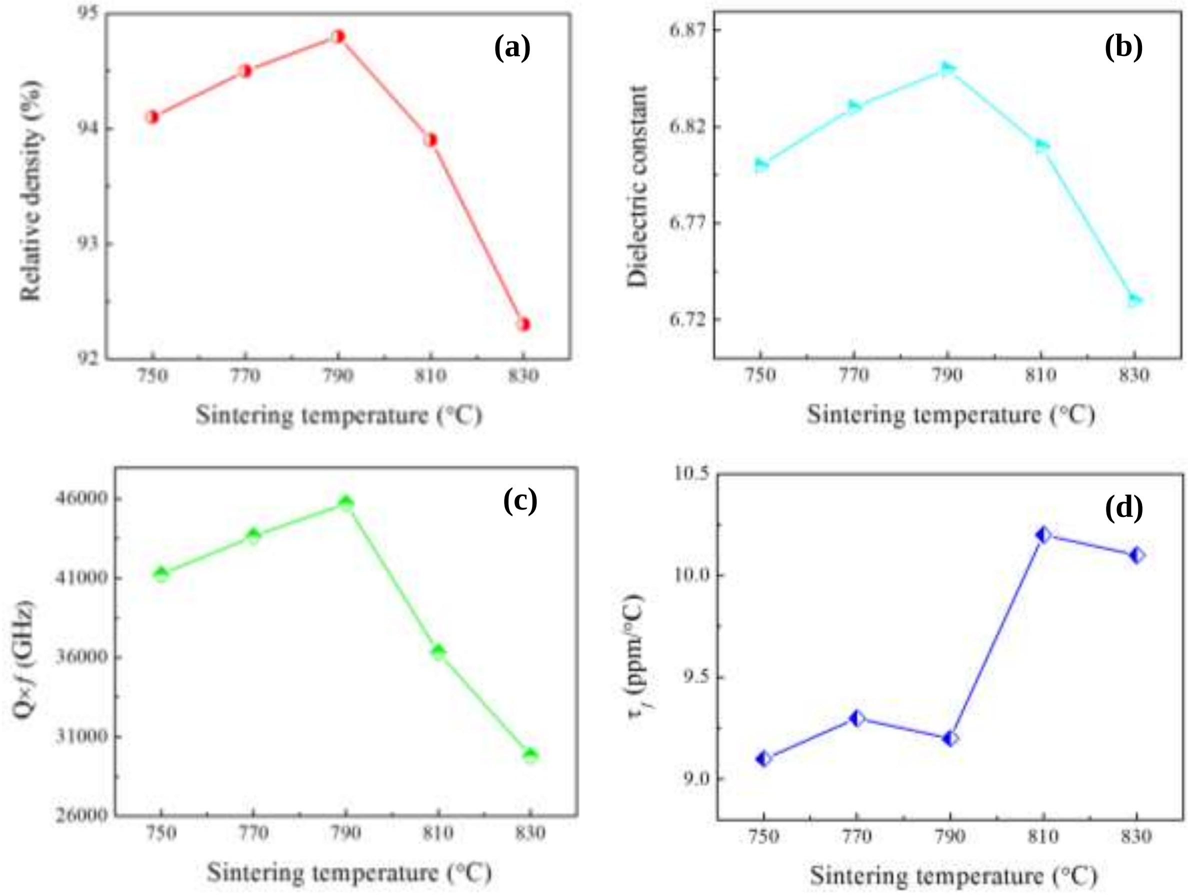

Figure S10 Apparent density (a), dielectric constant (b), quality factor (c) and temperature coefficient of resonant frequency (d) of the obtained $0.6Al_2Mo_3O_{12}$-$0.4TiO_2$ ceramics sintered at 750-830 °C for 12 h.

From **Figure S10**, it is seen that the apparent density reaches the maximum of 95.5% when the sample is sintered at 790 °C. Meanwhile, the dielectric constant and quality factor of the obtained $Al_2Mo_3O_{12}$ ceramics reach their maximum value, respectively. The temperature coefficient of resonant frequency of the obtained ceramics increased with increasing sintering temperature. Thus, from the point of microwave dielectric properties, 790 °C was the optimized sintering temperature for $0.6Al_2Mo_3O_{12}$-$0.4TiO_2$ ceramics.

Junqing Ren, et al., *Journal of Materials Chemistry C,* Figure S11

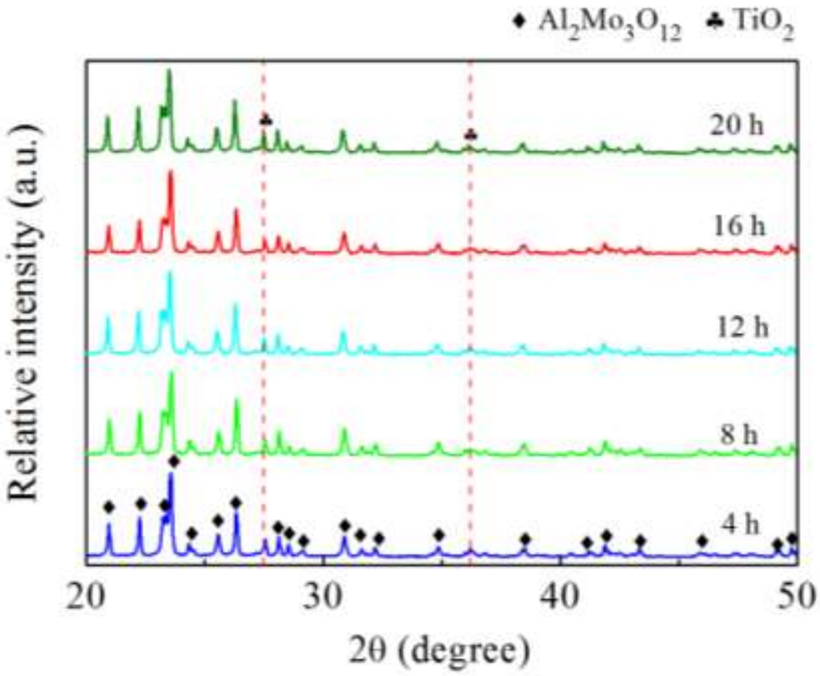

Figure S11 XRD patterns of the obtained $0.6Al_2Mo_3O_{12}$-$0.4TiO_2$ ceramics sintered at 790 °C for 4-20 h.

As is seen in **Figure S11,** monoclinic $Al_2Mo_3O_{12}$ (JCPDS card no. 84-1652) and rutile TiO_2 (JCPDS card no. 21-1276) phases could be detected in all the samples, indicating that TiO_2 could coexist with $Al_2Mo_3O_{12}$ phase. No other phases could be identified, when the samples were sintered at 790 °C.

Junqing Ren, et al., ***Journal of Materials Chemistry C*****, Figure S12**

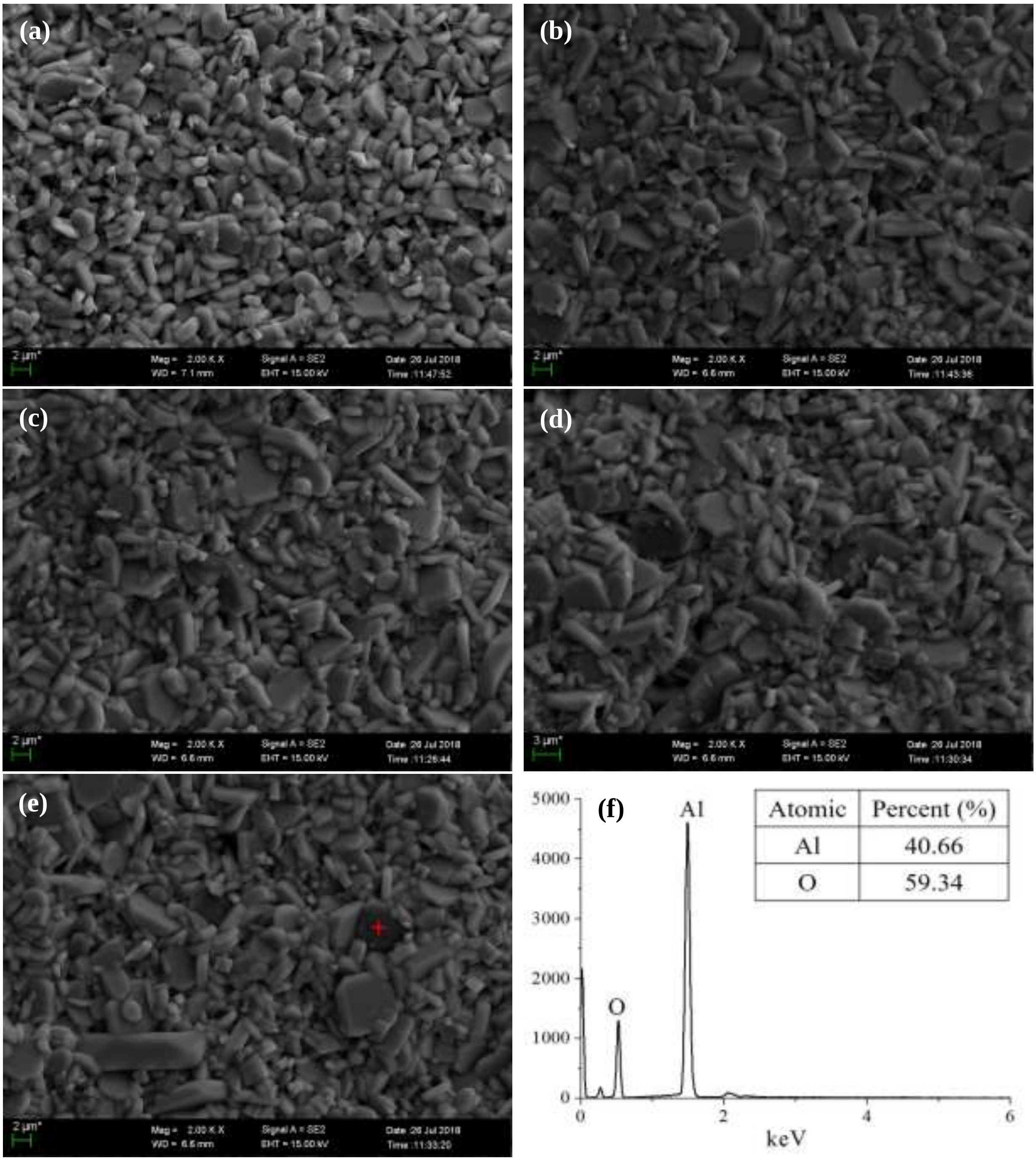

Figure S12 Typical SEM images of the obtained $0.6Al_2Mo_3O_{12}$-$0.4TiO_2$ ceramics sintered at 790 °C for different times: (a) 4, (b) 8, (c) 12, (d) 16, and (e) 20 h. (f) EDX data on the marked grain in (e).

As is seen in **Figure S12**, with the extension of sintering time, the average grain size of $Al_2Mo_3O_{12}$ increased. When sintering at 790 °C for a time shorter than 12 h, there exist inhomogeneously sized $Al_2Mo_3O_{12}$ grains and many pores in the samples. At 790 °C for 12 h, denser samples with more homogeneous grain size could be obtained. However, when sintering at 790 °C for a time longer than 12 h, some dark impurities consisting of Al_2O_3 appears in the samples together with the main $Al_2Mo_3O_{12}$ phase (see **Figure S12e**).

Junqing Ren, et al., *Journal of Materials Chemistry C*, Figure S13

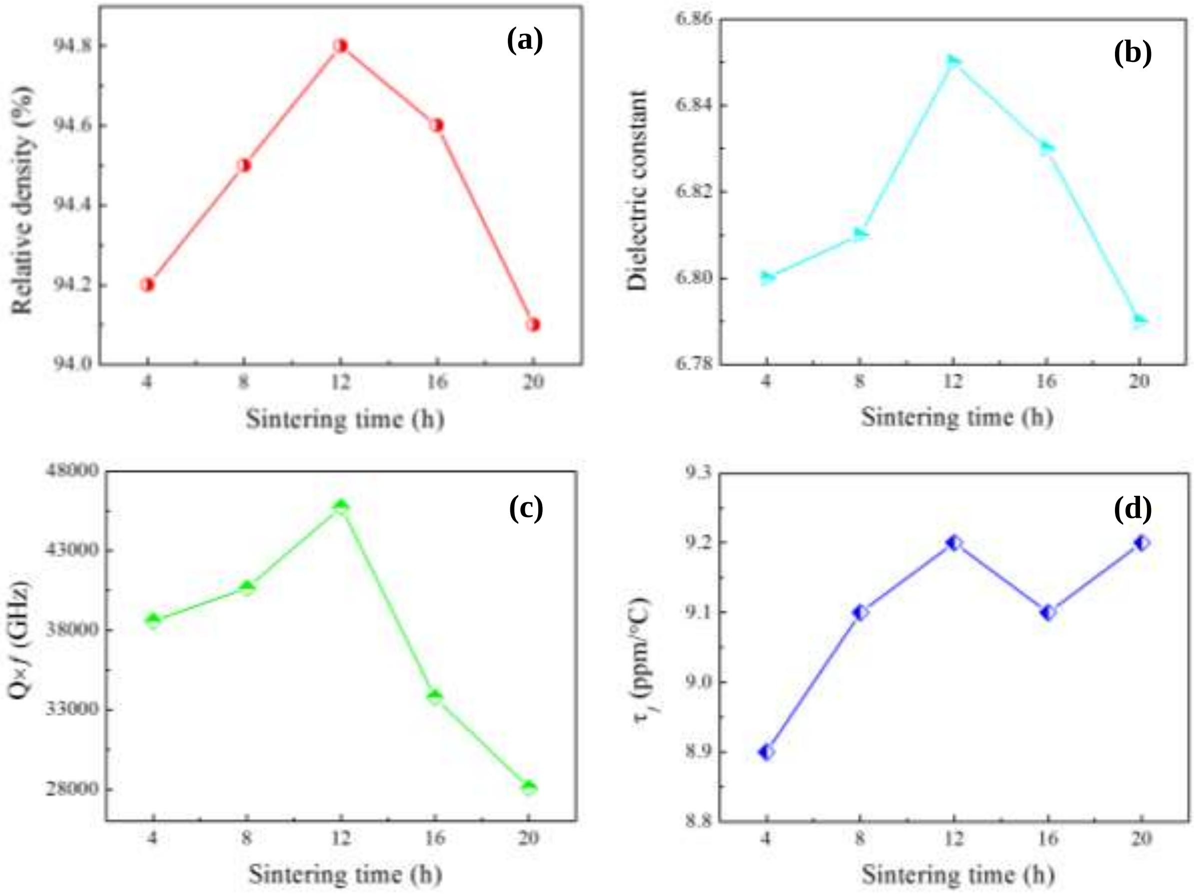

Figure S13 Apparent density (a), dielectric constant (b), quality factor (c) and temperature coefficient of resonant frequency (d) of the obtained $0.6Al_2Mo_3O_{12}$-$0.4TiO_2$ ceramics sintered at 790 °C for 4-20 h.

From **Figure S13**, it is seen that the apparent density reaches the maximum when the sample is sintered for 12 h at 790 °C. Meanwhile, the dielectric constant and quality factor of the obtained $Al_2Mo_3O_{12}$ ceramics reach their maximum value, respectively. The temperature coefficient of resonant frequency of the obtained ceramics increased with the time of sintering time. Thus, from the point of microwave dielectric properties, 12 h was the optimized sintering temperature for $0.6Al_2Mo_3O_{12}$-$0.4TiO_2$ ceramics.

In summary, $Al_2Mo_3O_{12}$ and $0.6Al_2Mo_3O_{12}$-$0.4TiO_2$ ceramics with the optimum microwave dielectric properties and highest density could be obtained at 790 °C for 12 h.

Junqing Ren, et al., *Journal of Materials Chemistry C*, Figure S14

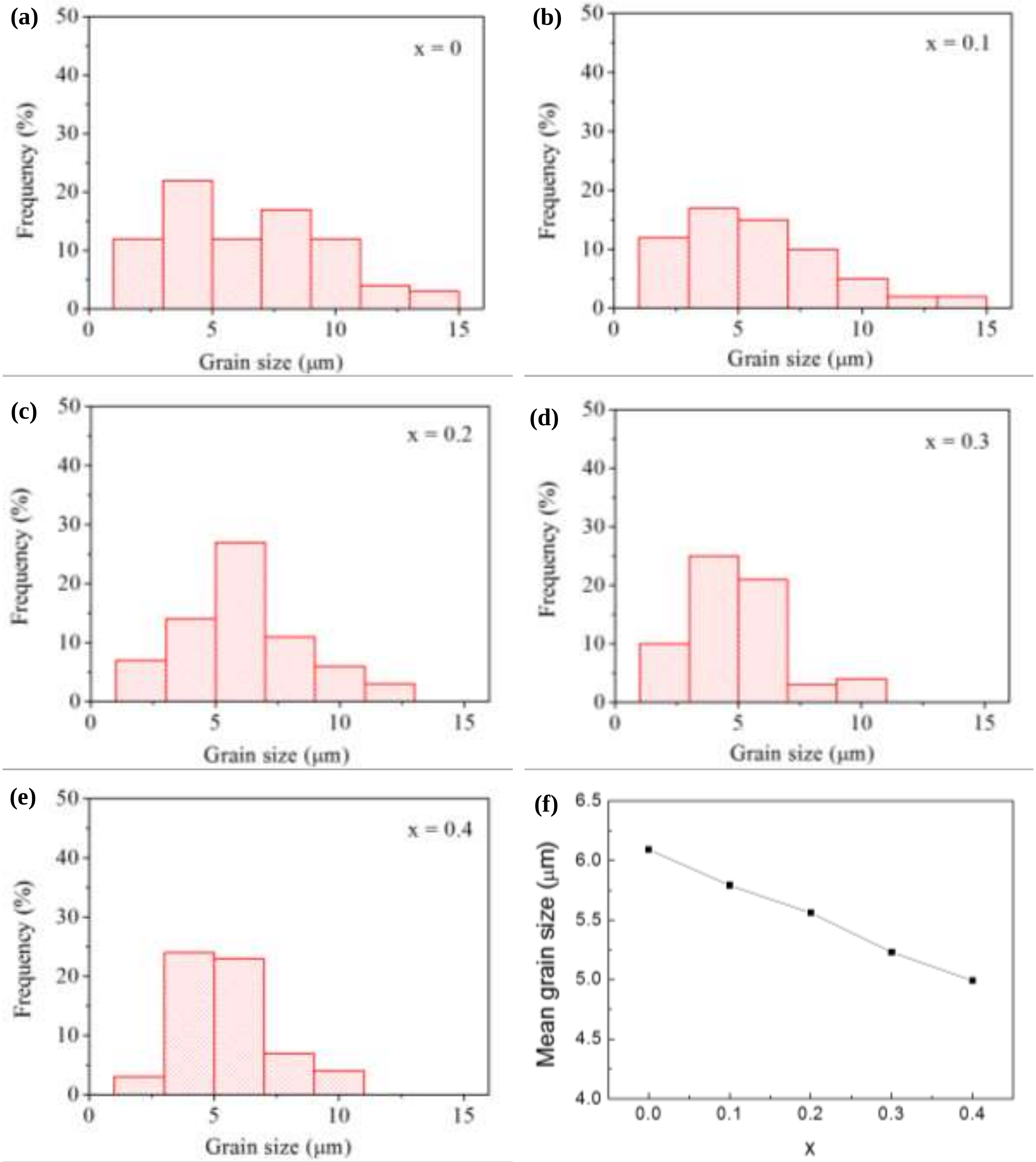

Figure S14 The grain size distribution of the obtained (1-x)$Al_2Mo_3O_{12}$-xTiO_2 ceramics sintered at 790 °C for 12 h with x=: (a) 0, (b) 0.1, (c) 0.2, (d) 0.3 and (e) 0.4. And (f) the average grain size of the (1-x)$Al_2Mo_3O_{12}$-xTiO_2 ceramics as a function of x value.

As is seen in **Figure S14**, with x from 0 to 0.4, the average size of $Al_2Mo_3O_{12}$ grain decreased from 6.09 to 4.9, indicating that the addition of TiO_2 could block the growth of $Al_2Mo_3O_{12}$ grains. Moreover, with increasing addition amount of TiO_2, the grain size distribution became more homogeneous.

Junqing Ren, et al., *Journal of Materials Chemistry C*, Figure S15

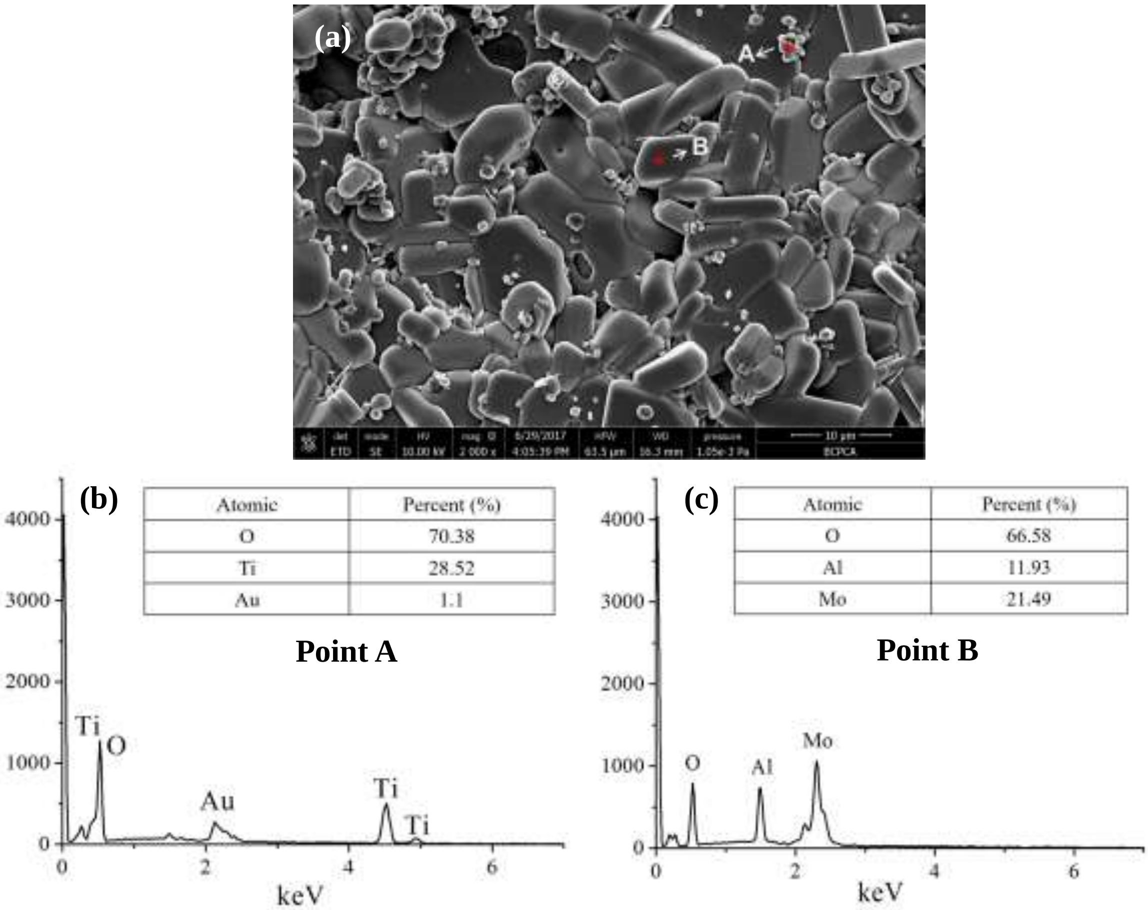

Figure S15 (a) Typical SEM image of the obtained $0.6Al_2Mo_3O_{12}$-$0.4TiO_2$ ceramics sintered at 790 °C for 12 h, and EDX data on the marked Points A (b) and B (c).

From **Figure S15**, it is seen that there are two kinds of color in the sample. The smaller white ones represent TiO_2 grains and the bigger grey ones shows $Al_2Mo_3O_{12}$ grains.